




Article

Urban Street Greening and Resident Comfort: An Integrated Approach Based on High-Precision Shadow Distribution and Facade Visual Assessment

Yuting Ni, Liqun Lin * , Huiqiong Xia  and Xiajun Wang 

Faculty of Resources and Environmental Science, Hubei University, Wuhan 430062, China; niyuting@stu.hubu.edu.cn (Y.N.); xhqiong2021@hubu.edu.cn (H.X.); 202221108012240@stu.hubu.edu.cn (X.W.)

* Correspondence: linliqun16@hubu.edu.cn; Tel.: +86-13317107235

Abstract: With the acceleration of global climate change and urbanization, the urban heat island effect has significantly impacted the quality of life of urban residents. Although numerous studies have focused on macro-scale factors such as air temperature, surface albedo, and green space coverage, relatively little attention has been paid to micro-scale factors, such as shading provided by building facades and tree canopy coverage. However, these micro-scale factors play a significant role in enhancing pedestrian thermal comfort. This study focuses on a city community in China, aiming to assess the thermal comfort of urban streets during the summer. Utilizing high-resolution 3D geographic data and street view images extracted from drone data, this study comprehensively considers the mechanisms affecting the urban street thermal environment and the human comfort requirements for shading and greening. By proposing quantitative indicators from multiple scales and dimensions, this study thoroughly quantifies the impact of the surrounding environment, greening, shading effects, buildings, and road design on the thermal comfort of summer streets. The results show that increasing tree canopy coverage by 10 m can significantly reduce the surrounding temperature, and a building layout extending 200 m can regulate temperature. The distribution of shadows at different times significantly affects thermal comfort, while the sky view factor negatively correlates with thermal comfort. Environments with a high green view index enhance visual comfort. This study reveals the specific contributions of different environmental characteristics to street thermal comfort and identifies factors that significantly impact thermal comfort. This provides a scientific basis for urban green space planning and thermal comfort improvement, holding substantial practical significance.

Keywords: city streets; thermal comfort; shading effect; UAV remote sensing data; trees and buildings



Academic Editors: Qi Feng and Tao Liu

Received: 6 January 2025

Revised: 21 January 2025

Accepted: 26 January 2025

Published: 27 January 2025

Citation: Ni, Y.; Lin, L.; Xia, H.; Wang, X. Urban Street Greening and Resident Comfort: An Integrated Approach Based on High-Precision Shadow Distribution and Facade Visual Assessment. *Sustainability* **2025**, *17*, 1026. <https://doi.org/10.3390/su17031026>

Copyright: © 2025 by the authors. Licensee MDPI, Basel, Switzerland. This article is an open access article distributed under the terms and conditions of the Creative Commons Attribution (CC BY) license (<https://creativecommons.org/licenses/by/4.0/>).

1. Introduction

Streets are a vital type of urban space, closely tied to residents' daily lives. In particular, pedestrian and cycling paths within cities, as key components of the slow traffic system, connect communities and surrounding areas, offering higher usage frequency and a more direct experience [1,2]. Against the backdrop of global climate change and the increasingly severe urban heat island effect, the thermal environment of urban streets during summer significantly impacts the quality of life for residents [3]. High temperatures and heat stress not only increase health risks for residents but also reduce the efficiency and comfort of urban spaces [4]. Building green streets is a crucial approach to enhancing street comfort.

Therefore, in areas severely affected by urban heat islands, assessing and optimizing the greening layout of summer streets is vital for alleviating thermal discomfort and creating more comfortable urban outdoor thermal environments. Comfort is the result of residents' combined psychological and physiological responses to the external street environment [5]. Therefore, the process of evaluating comfort involves a series of multidimensional and quantifiable indicators that reflect the complexity of the urban environment, people's psychological perceptions and physiological states, as well as their functional needs for urban slow traffic roads [6]. These indicators include factors such as air temperature [7], humidity, wind speed, solar radiation intensity, green coverage rate [8], tree shading effects, building shading effects, and street width. Consequently, identifying and characterizing the features of urban environmental complexity and residents' psychological and physiological needs that are closely related to the street thermal environment is crucial for assessing summer street comfort.

Previous studies have clearly demonstrated the positive impact of urban greenery on temperature regulation, improving the quality of life for urban residents, and enhancing street comfort [9–13]. However, traditional methods that use green coverage as an evaluation metric have significant limitations. These methods often consider only the overall greening rate without distinguishing between different types of vegetation such as trees, grass, and shrubs. Trees have a significantly better cooling effect compared to lower vegetation, but traditional assessments based on remote sensing data often mix trees with other vegetation, calculating green coverage based on two-dimensional information [14]. This approach fails to reflect the impact of different types of greenery on thermal comfort and overlooks the vertical dimension and spatial perception. For instance, the visual impact of greenery cannot be accurately captured by simple two-dimensional data, yet it greatly influences aesthetic quality and visual comfort.

Moreover, trees provide significant shading [15,16], which is crucial for summer street thermal comfort [17]. Tree shade can significantly mitigate the effects of solar radiation [18–20]. Research shows that tree shade during the day can reduce pedestrians' average body temperature by 2–3 °C compared to unshaded streets [18–20]. Tree shade also enhances the aesthetic quality of street views and affects people's physical activities [21]. Many cities worldwide have developed heat mitigation plans centered around street trees to improve thermal comfort for pedestrians and cyclists [22–24]. Traditional green space planning often involves symmetrically planting trees on both sides of streets, which, while aesthetically pleasing, does not fully consider the effectiveness of the greenery. This can leave pedestrians exposed to sunlight at critical times or cause them to alter their routes due to obstacles. Although extensive research has been conducted on the shading effects of different types of plants [25–27], using mathematical models of tree canopy shading to propose indicators such as cooling rates, shading rates, and shadow areas for quantitative analysis, these findings are challenging to directly apply to street comfort assessments and greenway planning at the community scale. Although it has long been recognized that exposure to solar radiation at the street level is a major cause of daytime thermal discomfort and that shading from buildings and trees can significantly reduce heat stress [6], there have been few attempts to quantitatively analyze solar radiation exposure at the urban scale. This is primarily due to the computational demands and limitations of high-resolution 3D geographic maps required for such analyses. Previous studies have explored the potential of using high-resolution shadow quantification and 3D urban mapping. Early research utilizing 3D GIS technology demonstrated the potential of 3D maps for calculating urban shadows [28]. With the development of drone technology and the acquisition of fine-scale Digital Surface Model (DSM) data, it is now possible to more accurately map and quantify

urban shading patterns, thus allowing for a better assessment of the impact of shading on urban thermal comfort.

Temperature is a key factor in assessing street thermal comfort. While quantifying the shading provided by buildings and trees can partially reflect human perception of the thermal environment, the mechanisms influencing street temperature extend beyond solar radiation shading effects and are also affected by surrounding environmental features. The micro-scale thermal environment in a city is influenced by multiple scales, and any single-scale evaluation method cannot fully capture the complexity of the urban environment. For instance, the shading effect of a single tree can significantly impact the thermal comfort of a specific sidewalk area, and this local detail can be clearly captured in small-scale evaluations. However, in larger-scale assessments, these local details are often overlooked, leading to inaccurate results. The temperature characteristics at any point on a street are influenced not only by nearby trees but also by surrounding green spaces and even the distribution of buildings on a larger scale. Therefore, evaluation methods lacking multi-scale analysis may provide incomplete or misleading assessments of thermal comfort. A fine-scale thermal environment assessment should encompass a multi-scale evaluation process.

2. Study Area and Data

2.1. Study Area

The study area is located in Wuhan, China ($30^{\circ}35' N$, $114^{\circ}17' E$), characterized by a typical subtropical monsoon humid climate with abundant sunshine and hot summers. The specific study site is the Xujiapeng community in Wuhan (Figure 1). This area covers approximately 7.6 square kilometers, with a dense population and a mix of residential and commercial zones, representing a typical urban community.

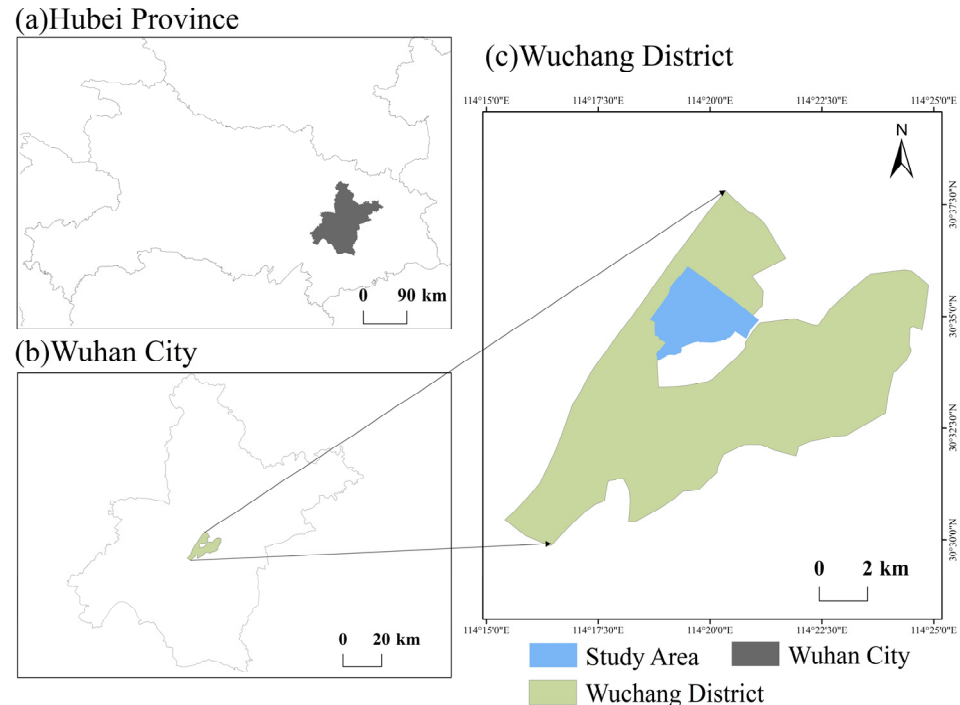


Figure 1. Overview of the research area.

In this study, 108 pedestrian street segments and 102 cycling street segments were selected as research samples within the Xujiapeng community. These segments represent various types of urban streets and diverse environmental features, including residential areas, commercial zones, public facilities, and urban parks.

2.2. Data Sources

The dataset used in this study (Table 1) primarily covers four categories: drone data, urban road network data, and street view image data. The drone data were collected in October 2021 using a DJI M300 RTK (Dajiang technology, Shenzhen, China) equipped with a ZENMUSE P1 lens ($f = 35$ mm). Vertical imagery was captured with a longitudinal overlap of 80% and a lateral overlap of 70%. The flight took place at an absolute altitude of 500 m, covering a ground area of 7 km². After the flight, the data were processed using DJI Terra software (DJI Terra V3.3.0) to obtain high-resolution Digital Orthophoto Maps (DOMs) and high-precision DSM for the study area. The detailed extraction process can be found in Lin et al. [29]. These data provide key information about buildings, trees, and roads, including the distribution and height of buildings, the location and canopy of trees, and the distribution and width of roads, with distinctions made between cycling paths and sidewalks.

Table 1. Dataset.

Data Type	Format	Data Sources	Data Usage
DOM DSM	TIF	DJI-M300 RTK Drone	Calculate tree ratio (Tree), building ratio (Build), shadow coverage (SC), sky view factor (SVF), and shade status (Shade)
Road Surface	Shape File	DOM Visual Interpretation	Distinguish between pedestrian paths and cycling paths, and calculate the road width (Width)
Road Sampling Points		OSM	Used to obtain street views in Baidu Maps
Baidu Street View (BSV)	JPEG	Baidu Maps	Calculate green view index (GVI)
Measured temperature data	Excel	Omega H3009	Determine the research scale

The street view data were obtained from Baidu Maps, while the urban road network data were sourced from OpenStreetMap (OSM). Sampling points were set every meter along the streets in the study area, resulting in a total of 8067 sampling points. Using these points, street view images from May 2019 were collected, capturing four angles at each point to create 360° panoramic views, providing detailed facade visual information.

The measured air temperature data were collected over three days: 29 August, 30 August, and 17 September 2021. A temperature recorder (Omega H3009) and GPS were used simultaneously to record the temperature and location at different points in four regions. During data collection, each temperature reading was labeled as either being in direct sunlight or in the shade. The temperature sensor was placed 0.8 m above the ground, and to ensure accurate readings, it was left stationary for 1 min under calm wind conditions before recording the temperature data.

3. Methods

This study aims to evaluate the comfort of streets in an urban community (7 square kilometers) by combining thermal comfort and visual perception characteristics. First, detailed temperature measurements and drone data collection were conducted in the city center to calculate environmental features related to thermal comfort. By computing various climate and morphological variables, we identified environmental scales and characteristics associated with summer thermal comfort levels. Next, we analyzed the shading levels of all street segments in the area, distinguishing between pedestrian paths and cycling paths. The Urban Multi-Scale Environmental Predictor (UMEP) [30] tool (UMEP Ltd., Phnom Penh, Cambodia) was used to calculate the three-dimensional visual perception characteristics of analysis units. Semantic segmentation of the street view data was employed to extract

the three-dimensional visual perception features of these units. Additionally, the street width for each evaluation unit was calculated based on vector data for cycling paths and pedestrian paths. Finally, the Analytic Hierarchy Process–Technique for Order of Preference by Similarity to Ideal Solution (AHP-TOPSIS) was used to determine a greenway comfort evaluation map. This map will assist in prioritizing future municipal actions to achieve optimal shading protection and spatial efficiency.

3.1. Multi-Dimensional and Multi-Scale Indicators and Evaluation Units

This study establishes a multidimensional, multi-scale evaluation system for comprehensively assessing the thermal comfort of urban streets during summer. The system includes three primary indicators and six secondary indicators (Table 2), aiming to ensure comprehensive and accurate evaluations by integrating environmental, psychological, and functional needs.

Table 2. Indicator system.

Primary Index	Secondary Index	Calculation Method and Explanation
Environmental dimension	Tree *	Evaluation unit is 1 m and 5 time scales.
	Build *	Evaluation unit is 1 m and 5 time scales.
	GVI	Evaluation unit is 1 m and at point level and road line level.
	SC *	Intersection tabulation; evaluation unit is 1 m and 5 time scales.
Dimensions of physical and mental needs	SVF	$SVF = \sum_{i=1}^n S \frac{2}{2\pi} \sin\left(\frac{\pi}{180}\right) \sin\left(\frac{\pi(2\alpha_i-1)}{2n}\right) \frac{360}{\theta_i}$ where S is the Boolean image of the shadow pattern, n is the total number of shadow maps generated, α_i is the altitude angle in degrees, and θ_i is the number of azimuth angles used at the i ring level. Evaluation unit is 1 m.
	Shade Width	Evaluation unit is 1 m and 5 time scales. Evaluation unit is 1 m.

* Indicates multi-scale characteristics.

In the environmental dimension, the secondary indicators are tree coverage and building coverage. Tree coverage refers to the proportion of area covered by tree canopies within a specific buffer zone. Trees not only provide greenery but also significantly impact local temperatures through shading and transpiration. Building coverage refers to the proportion of the area occupied by buildings within a specific buffer zone. The shading effects and heat capacity of buildings play a crucial role in street temperature regulation.

Secondly, the physical and mental needs dimension includes four secondary indicators: GVI, SC, SVF, and Shade. GVI measures the visible proportion of green vegetation from a pedestrian's viewpoint at a sampling point, significantly affecting visual comfort and psychological relaxation. Shadow coverage is the proportion of actual shadow-covered area within a certain range at a sampling point, which can significantly reduce overall air temperature in that area. SVF is the visible proportion of the sky at a 1 m sampling point, influencing solar radiation reception and thermal environment. Shading status evaluates whether the sampling point is under direct sunlight or shade, assessing the quality and distribution of shade and its impact on pedestrian thermal comfort.

Finally, the functional requirement dimension includes the width of cycling/pedestrian paths. Spacious pedestrian and cycling paths not only improve traffic fluidity and convenience but also enhance the sense of safety and comfort of users.

Since the street view data are sampled at 1 m intervals, subsequent indicator evaluation units are also set to 1 m to ensure accuracy and consistency. Combining studies on the impact of different spatial scales on thermal comfort, such as Lin et al. [29], highlighting that tree canopy area within 10–20 m significantly affects micro-scale temperatures, and Lan and Zhan [31], identifying 200 m as the optimal scale for analyzing the relationship between air temperature and building configuration, the final street scale for reflecting the thermal environment is determined to be 10 m and 200 m.

3.2. Shadow Extraction

To accurately capture the dynamic changes in shadows caused by urban buildings and trees, this study utilized UMEP on the open-source GIS platform QGIS. The analysis employed DSMs of the ground and buildings for pixel-by-pixel shadow generation. To enhance accuracy, the DSM of the vegetation canopy was also included. Notably, the shadows of tree trunks vary with the solar altitude angle, and neglecting them may introduce errors in shadow analysis. Based on field surveys of building and tree distributions in the study area, the plant transmissivity was set to 0%, and the tree canopy coverage was assumed to be 50%. Using the DSMs of the ground, buildings, vegetation canopy, wall height, and slope data, shadow distribution maps were generated for five different times on September 1, 2021 (8:00, 10:00, 12:00, 14:00, 16:00).

In these shadow distribution maps, areas shaded by buildings were assigned a value of 0, areas shaded by trees a value of 0.1, and areas fully exposed to sunlight a value of 1. For ease of analysis, the shadow results were reclassified, with 1 representing shaded areas and 0 representing unshaded areas.

To further estimate the shading coverage for pedestrians and cyclists, this study used street network data. Buffers were created around the center points of the roads, with each road's width determining the buffer size, generating road polygons. These polygons were then overlaid with the shadow maps for each time point. Intersection analysis was used to calculate the shading coverage for each road segment at different times. Additionally, this method accurately determined the contributions of buildings and trees to shading at a 1 m spatial scale.

3.3. Street View Data Processing: Calculation of Green View Index

This study employs deep learning algorithms to apply semantic segmentation at the pixel level for processing street view images, enabling the automatic classification of street greenery [32]. This method utilizes semantic segmentation models to extract street greenery information [11,33] and calculate the GVI, reflecting the actual visual exposure of residents to greenery.

First, street view images collected from four directions are stitched together into a panoramic image. Then, deep learning is used to perform semantic segmentation on the panoramic street view image, automatically extracting object elements. These elements include landscapes (such as sky, grass, ground), natural features (such as shrubs, trees, water bodies), and artificial features (such as buildings, bridges, roads), as well as smaller urban elements (such as cars, bicycles). After obtaining detailed semantic segmentation results, the GVI is calculated. This index is derived from the sum of the percentage areas of six plant recognition features (palm, trees, plants, grass, and flowers). By processing street view data, the GVI indicator, which reflects real environmental facade information, is extracted.

3.4. Calculation of Road Width

To achieve precise street width measurement, this study combines GIS and programming to calculate the street width for each evaluation unit (1 m intervals). Using ArcGIS

software (ArcGIS 10.8) tools, the street width is calculated at 1 m intervals along the road axis by setting cross-sectional profile lines. The specific process is as follows (Figure 2).

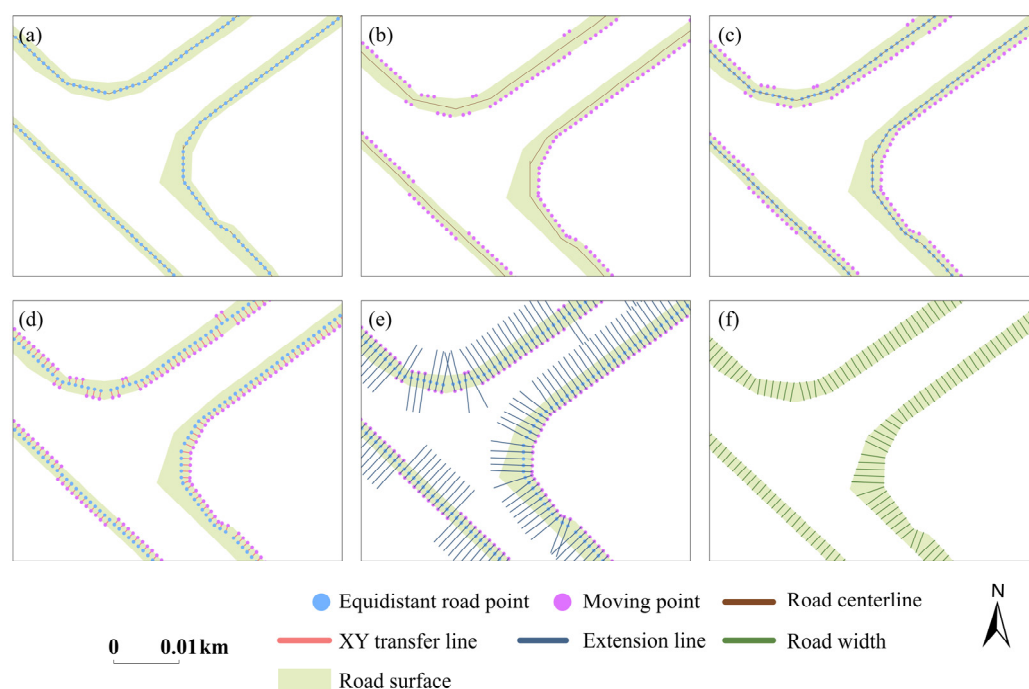


Figure 2. (a) Sampling points with an equal distance of 1 m generated by road lines. (b) Use point line topology tools to move points to the nearest boundary from the road route. (c) Move the position of the front and rear points. (d) XY transfer line. (e) Extend the line segment. (f) Cropping with road surface.

Sampling point generation: in ArcGIS, create equidistant sampling points (every 1 m) for cycling paths and pedestrian paths, and import accurate data of the road boundaries.

Point–line topology analysis: Develop a custom Python script to perform point–line topology analysis, determining whether each sampling point is precisely located on the road boundary line. If a sampling point is not aligned, the program will automatically adjust the point to the nearest boundary line, ensuring it is correctly positioned.

Position change recording: Use the attribute table join function to record the specific position changes of each road point before and after adjustment, ensuring the integrity of point position data. Convert these points into line segments.

Street width calculation: use the extend line tool in QGIS to accurately trim the generated line segments with the road boundaries, calculating the street width for each evaluation unit.

3.5. AHP and TOPSIS

This study employs the AHP and the TOPSIS to determine the weights of various indicators in the urban community street thermal comfort evaluation system. The AHP is used to establish the hierarchical structure of evaluation indicators and assign weights to reflect their relative importance in the assessment. Then, the TOPSIS method is utilized to evaluate each road point based on the indicator weights, and the scores of these points are averaged to calculate the overall road score. The process includes constructing a hierarchical model, calculating indicator weights, applying the TOPSIS evaluation, and ranking the road points based on their scores. By combining the AHP and TOPSIS methods, relatively reliable indicator weights can be obtained, allowing for a comprehensive assessment of the thermal comfort of urban community streets.

4. Research Results

4.1. Quantitative Indicators Related to Thermal Comfort

The drone data processing resulted in a DOM with a resolution of 4.7 cm and a DSM with a resolution of 9.4 cm and an elevation accuracy of 0.5 m, as shown in Figure 3a,b. Tree canopy distribution data, building height data, and land cover data are shown in Figure 3c to Figure 3e, respectively.

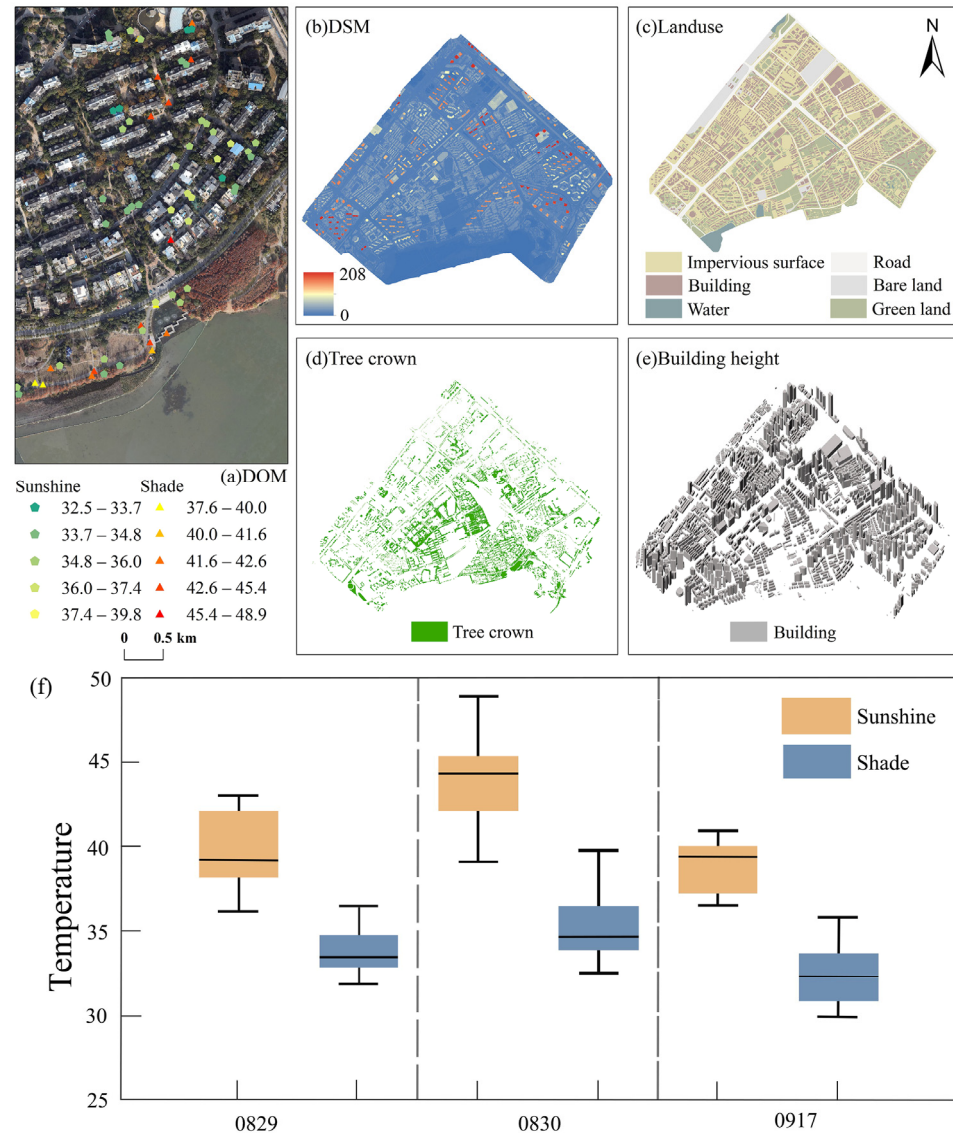


Figure 3. Drone data processing.

When selecting quantitative indicators related to thermal comfort, it was considered that buildings and trees are the primary sources of urban shading. Therefore, this study focused on the impact of building and tree coverage at different scales on temperature. This research used a DSM, a DOM, and temperature data to establish 17 buffer zones around each temperature measurement point, ranging from 2.5 m to 500 m, covering multiple scales. By visualizing land cover using DOM data, two key parameters—building and tree canopy coverage—were extracted for 10 m and 200 m ranges. Significant temperature variations between sunlit and shaded areas were observed in urban regions (Figure 3a). Statistical analysis using ANOVA revealed significant temperature differences between sunshine and shade during all three sampling periods ($p < 0.01$, Figure 3f).

The results of multiple linear regression analysis (Table 3) showed adjusted R^2 values of 0.825, 0.843, and 0.834, indicating a good model fit and the ability to effectively reflect the impact of land cover on temperature at different scales. Specifically, the coefficients for buildings at the 200 m scale were positive, at 0.062, 0.059, and 0.069, with t -values significantly greater than 5, indicating a significant positive influence of buildings on temperature at larger spatial scales. On the other hand, at the 10 m scale, the correlation coefficients for tree canopy coverage were negative, at -0.019 , -0.014 , and -0.019 , with t -values significantly less than -4 , showing a cooling effect of tree canopy coverage at smaller scales.

Table 3. Stepwise regression results.

Date	R^2	Building 200 m Coefficient (B)	Building 200 m Significance (T)	Canopy 10 m Coefficient (B)	Canopy 10 m Significance (T)
0829	0.825	0.062	6.779	-0.019	-4.435
0830	0.843	0.059	5.190	-0.014	-4.316
0917	0.834	0.069	5.269	-0.019	-4.559

In summary, the influence of tree canopy coverage within a 10 m range and buildings within a 200 m range on temperature is particularly significant. The findings indicate that buildings have a positive impact on thermal comfort at larger scales by providing shade and modulating wind direction, while tree canopy coverage positively affects thermal comfort at smaller scales through cooling and improving air quality. Based on these analyses, tree and building parameters within these scale ranges are selected as key indicators for subsequent thermal comfort evaluation.

4.2. Shadow Analysis Results

In evaluating the summer street comfort of urban communities, the UMEP model was used to calculate shadow distribution at a resolution of 1 m per pixel, providing a crucial basis for assessing street comfort throughout the day. According to the method described in Section 3.2, shadow calculations were performed every 2 h to capture dynamic changes over time. As a result, shadow distribution data were obtained for five different time points: 8:00 AM (Figure 4a), 10:00 AM (Figure 4b), 12:00 PM (Figure 4c), 2:00 PM (Figure 4d), and 4:00 PM (Figure 4e).



Figure 4. Distribution map of building and tree canopy shadows at different times.

The 8:00 AM shadow analysis helps to understand the coolness of the streets at the start of the day, while the 10:00 AM analysis shows the trend of shadow changes in the morning. The 12:00 PM analysis evaluates shadow distribution during the hottest part of the day, crucial for ensuring pedestrian comfort under high temperatures. The 2:00 PM and 4:00 PM analyses further reveal shadow changes in the afternoon and early evening, important for assessing street comfort as the day progresses.

Plotting the average shadow coverage at the street level (Figure 5) shows significant differences in shading among various streets within the study area. The analysis indicates that at 8:00 AM (Figure 5a), some roads have higher shadow coverage, while others have relatively low coverage. This disparity is primarily due to the shadows cast by tall buildings or trees under low-angle sunlight. During this time, because the angle between the sunlight and the ground is smaller, shadows are generally longer, meaning that even areas not directly under the sun may enjoy higher shadow coverage.

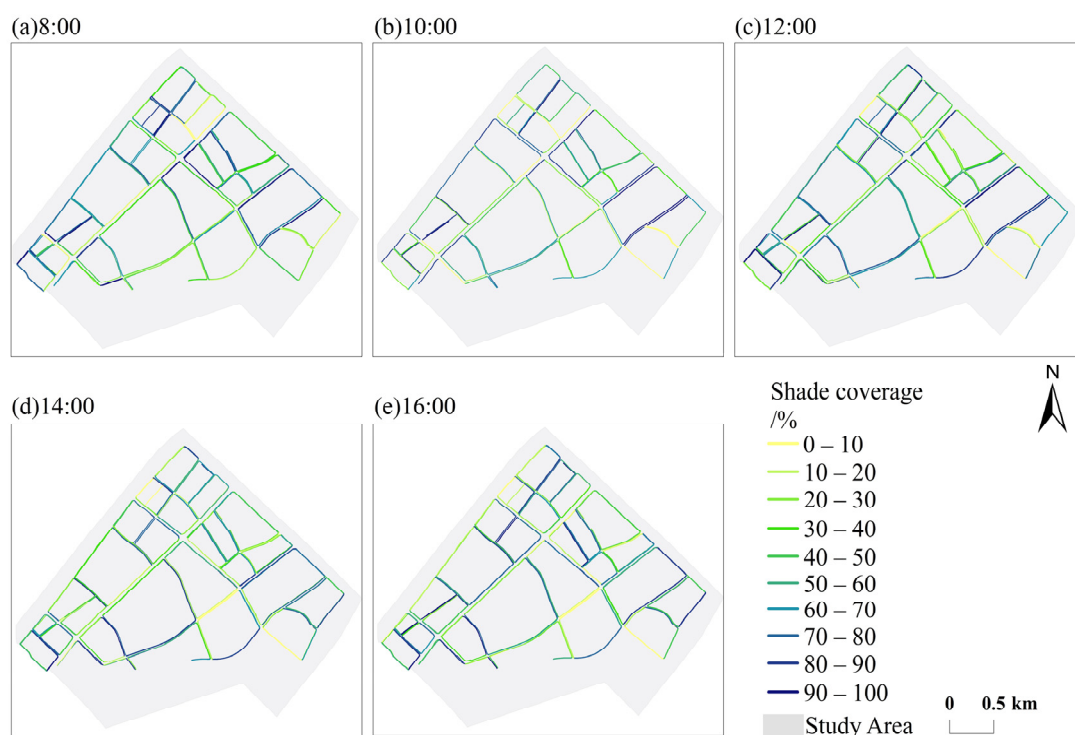


Figure 5. Distribution map of shading coverage at each moment.

At 10:00 AM (Figure 5b), as the sun's altitude increases, shadows become shorter but more pronounced, though still longer than at noon. At this time, shadows start to recede from the west side of buildings and trees, affecting the shading range on the streets and causing shadow coverage in some areas to decrease.

At noon (Figure 5c), when the sun is at its highest point, shadows are at their shortest, tightly hugging the base of buildings and trees. Because the shadows are short and vertical, their shading effect on the roads is less effective compared to morning or evening.

At 2:00 PM (Figure 5d), as the sun moves westward, shadows become longer again, extending towards the northeast. Compared to noon, shadows are more significant, providing more shade for pedestrians.

At 4:00 PM (Figure 5e), the sun continues its descent towards the west, and shadows extend further to the east, increasing in length compared to noon. During this time, some streets may exhibit higher shadow coverage, offering a cooler and more comfortable environment for pedestrians.

4.3. Visual Perception-Related Features: Sky View Factor

The SVF measures the openness of the sky, ranging from nearly 0 (indicating severe obstruction) to 1.0 (indicating complete openness). Analyzing the SVF distribution map (Figure 6), the average SVF value in the study area is 0.74, indicating a generally high level of sky openness. However, many SVF values are low due to high-rise residential buildings and street trees that block the sky, forming narrow street canyons.

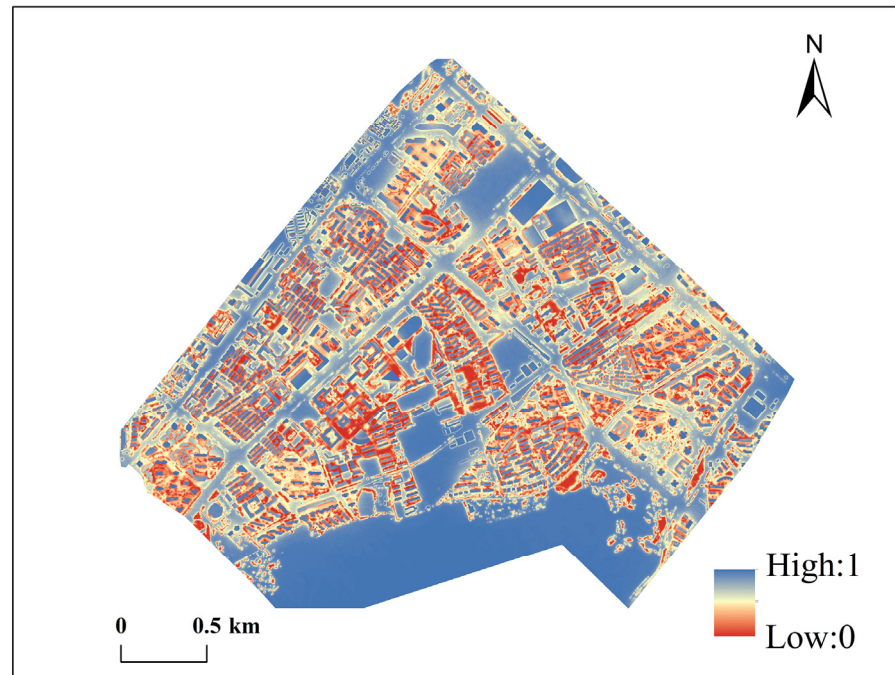


Figure 6. SVF calculated using the UMEP model.

In contrast, areas with higher SVF values likely have shorter or more sparsely distributed buildings, resulting in a more open landscape. This openness provides residents with a more comfortable outdoor environment and promotes natural light and air circulation. Further analysis reveals that streets with tall, densely packed buildings have lower SVF values, reflecting the concentration of high-rise buildings and urban density. The density of buildings not only affects the visual perception of the cityscape but also significantly impacts air circulation, directly influencing the thermal comfort of urban streets.

4.4. Visual Perception-Related Features: GVI

GVI extracted from street view images is a crucial metric for measuring urban greening levels. The street network of the study area was obtained from OSM, with sampling points set at 1 m intervals along each road. A total of 8408 sampling points with coordinates were identified, and street view images for these points were downloaded.

Using the method described in Section 3.4 (Figure 7), the greening level of streets in the study area was quantified. According to Natsuki Oryu's classification [34], GVI can be divided into five levels: non-green (0–0.05), low green (0.05–0.15), moderately green (0.15–0.25), green (0.25–0.35), and very green (0.35–1). Figure 7c shows the GVI distribution, revealing significant spatial heterogeneity. Areas with a high GVI are well greened, enhancing residents' visual experience and providing diverse ecosystem services. Conversely, areas with a low GVI lack sufficient vegetation, indicating a need for improved greening. Regions with a moderate GVI are distributed across various parts of the study area, reflecting uneven urban greening across different streets.

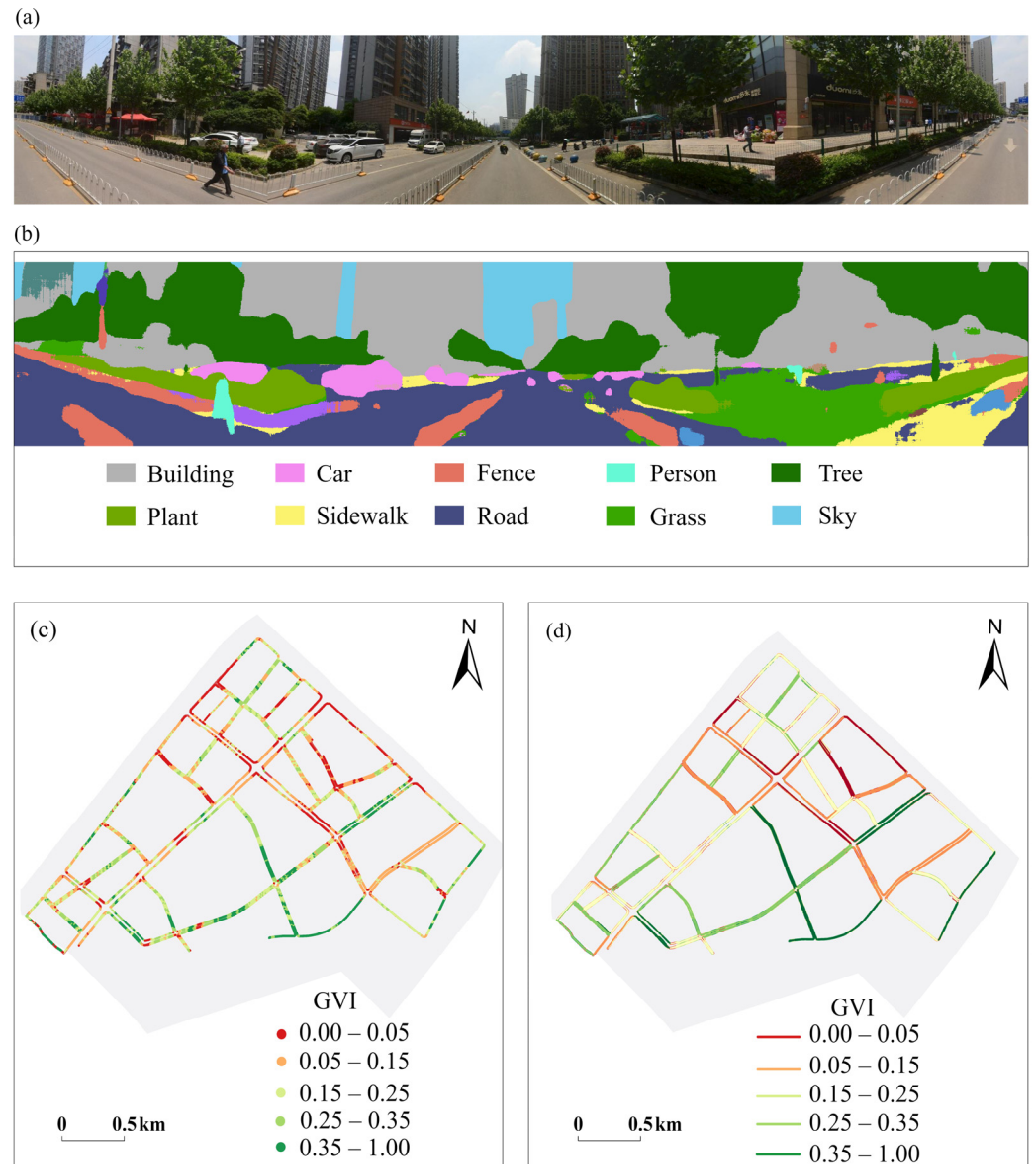


Figure 7. (a) Street view image. (b) The results of semantic segmentation. (c) Distribution map of GVI results (point level). (d) Distribution map of GVI results (road level).

Figure 7d further illustrates the GVI distribution at the road level, showing spatial variations in the average GVI. Some roads, while not having a high overall GVI, may have concentrated green areas or nodes. Although the overall GVI levels of road spaces are not high, there are differences in GVI levels at individual points within the road space.

The results reveal the statistical characteristics and spatial distributions of street greening, accurately quantifying greening from a human-centered perspective. Evaluating the GVI based solely on observation points does not provide a comprehensive assessment of road space comfort. Therefore, to fully assess the comfort of road spaces, the GVI must be considered along with other relevant factors.

4.5. AHP-TOPSIS Indicator Weight

Using the AHP, we calculated the weights of factors influencing the summer comfort of urban community streets under residents' travel needs. The weights were derived using the AHP online calculator. To ensure the scientific rigor and accuracy of the weight determination, this study integrated expert opinions, a literature review, and the characteristics

of the study area in the process. A pairwise comparison matrix was then constructed, and the consistency of the results was verified. The consistency ratio was calculated to be 0.015 (<0.1), indicating that the judgments are consistent. These varying weights of evaluation factors provide a basis for assessing the different comfort levels of streets (Table 4).

Table 4. Weight values of relevant indicators.

Target Layer	Indicator Layer	Comprehensive Weight
Road Comfort Level	Shade	0.2604
	SC	0.3991
	Build	0.0806
	Tree	0.0998
	GVI	0.0454
	SVF	0.0874
	Width	0.0273

Table 3 shows that the highest weights were assigned to SC (0.3991) and Shade (0.2606), followed by Tree (0.0998), SVF (0.0874), and Build (0.0806). The lowest weights were assigned to GVI (0.0454) and Width (0.0273). After assigning appropriate weights using the AHP method, the TOPSIS method was applied on the SPSS software (IBM SPSS Statistics 27.0) platform to calculate the comprehensive score C based on distance values, and the results were ranked accordingly. The classification results from the TOPSIS method were exported as a text file and imported into ArcGIS 10.8. Using the natural breaks (Jenks) classification method [35], the scores were categorized into five levels (Figure 8): very low comfort, low comfort, moderate comfort, high comfort, and very high comfort.

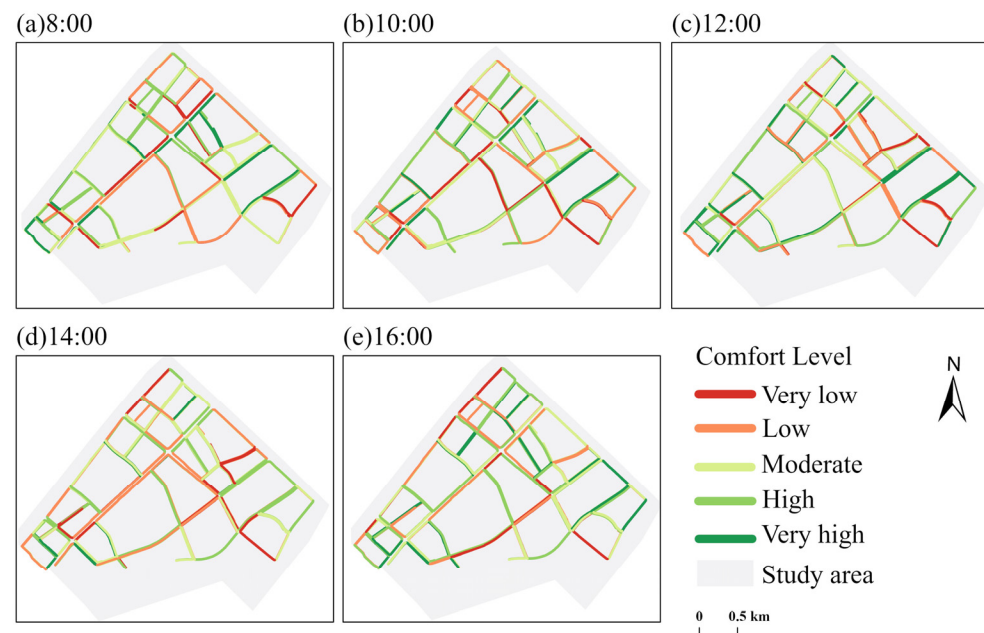


Figure 8. Road distribution map of comfort at different time points.

Through the scoring system, the thermal comfort performance of each road at different time points can be assessed, and roads can be categorized into different levels of comfort based on their scores. Higher scores indicate better thermal comfort at the corresponding time points.

4.6. Thermal Comfort Evaluation of Community Road

This study aims to propose scientifically reasonable street optimization plans by comprehensively considering factors affecting thermal comfort at different times of the day. Based on multi-period thermal comfort data, a comprehensive evaluation table for each time period was established (Table 5). The weight distribution is based on the intensity of sunlight and the duration of outdoor activities at different times of the day.

Table 5. Weight values for each time.

Time	Weight
8:00	0.2
10:00	0.18
12:00	0.15
14:00	0.2
16:00	0.27

The thermal comfort scores for each time period were weighted and combined according to the assigned weights, resulting in a comprehensive evaluation score (Figure 9). This score reflects the overall thermal comfort level of the streets throughout the day.



Figure 9. Distribution chart of comprehensive scores for comfort at different time points.

The comfort of cycling and pedestrian paths varies throughout the day, likely due to changes in the sun's position and the dynamic distribution of environmental shadows. As the day progresses, especially around noon, the comfort of these paths tends to decrease due to increased solar radiation intensity. During this time, the shade provided by trees and buildings plays a crucial role, helping to maintain lower surface temperatures and providing necessary shelter for pedestrians and cyclists.

It is noteworthy that in areas with more shade, both cycling and pedestrian paths generally offer higher levels of comfort. This is because shade effectively reduces the heat load from direct sunlight. Additionally, the placement of these paths is closely related to the density of surrounding buildings and the width of the roads, which together influence air circulation and shadow distribution patterns. For example, pedestrian paths may be located closer to buildings or on narrower streets, while cycling paths might be situated on wider roads. These locational differences lead to varying thermal comfort experiences.

In areas with a high GVI and low SVF, although trees provide a comfortable microclimate, excessive canopy coverage can limit sky visibility, affecting people's perception of thermal comfort.

To quantify the correlation between thermal comfort and these seven variables, Pearson correlation coefficients (r) were calculated. Table 6 reports these coefficients, showing the degree of association. Build200m (building proportion within 200 m), Tree1m (tree proportion within 1 m), Tree10m (tree proportion within 10 m), Shade, SC, GVI, and Width are significantly positively correlated with thermal comfort scores (Grade), with r values of 0.112 ($p = 0.01$), 0.386 ($p = 0.01$), 0.602 ($p = 0.01$), 0.284 ($p = 0.01$), 0.802 ($p = 0.01$), 0.202 ($p = 0.01$), and 0.03 ($p = 0.01$), respectively. On the other hand, SVF is negatively correlated with thermal comfort scores ($r = -0.436$, $p = 0.01$).

Table 6. Pearson correlation between evaluation indicators and street thermal comfort ($n = 84,420$).

	Build 200m	Tree 1m	Tree 10m	Shade	SC	GVI	SVF	Width	Grade
Build 200m	1 (0.000 ***)								
Tree 1m	0.003 (0.364)	1 (0.000 ***)							
Tree 10m	-0.026 (0.000 ***)	0.021 (0.000 ***)	1 (0.000 ***)						
Shade	-0.01 (0.005 ***)	0.173 (0.000 ***)	0.015 (0.000 ***)	1 (0.000 ***)					
SC	0.015 (0.000 ***)	0.007 (0.058 *)	0.638 (0.000 ***)	0.02 (0.000 ***)	1 (0.000 ***)				
GVI	-0.012 (0.000 ***)	0.248 (0.000 ***)	-0.015 (0.000 ***)	0.104 (0.000 ***)	-0.011 (0.001 ***)	1 (0.000 ***)			
SVF	-0.007 (0.053 *)	-0.626 (0.000 ***)	-0.025 (0.000 ***)	-0.419 (0.000 ***)	-0.04 (0.000 ***)	-0.257 (0.000 ***)	1 (0.000 ***)		
Width	0.055 (0.000 ***)	0.002 (0.654)	-0.04 (0.000 ***)	0.036 (0.000 ***)	-0.002 (0.636)	-0.018 (0.000 ***)	-0.077 (0.000 ***)	1 (0.000 ***)	
Grade	0.112 (0.000 ***)	0.386 (0.000 ***)	0.602 (0.000 ***)	0.284 (0.000 ***)	0.802 (0.000 ***)	0.202 (0.000 ***)	-0.436 (0.000 ***)	0.03 (0.000 ***)	1 (0.000 ***)

***, and * represent significance levels of 1%, and 10%, respectively.

The following results can be summarized:

1. Build200m and Tree10m: There is a weak negative correlation (-0.026), indicating that on a larger scale, an increase in buildings might slightly negatively impact the proportion of trees. This may be due to the competition between building land and green space in the urbanization process.
2. Shade and Tree1m: there is a significant positive correlation (0.173), suggesting that the presence of trees increases shaded areas, which can enhance thermal comfort, especially during hot summers.
3. SC and Tree10m: there is a strong positive correlation (0.638), indicating that within a smaller range (10 m), the number of trees is closely related to shadow coverage, further confirming the important role of trees in providing shade and reducing temperature.
4. GVI and Tree1m: there is a significant positive correlation (0.248), indicating that an increase in trees can significantly enhance the green visual experience, which may positively impact residents' psychological comfort.
5. SVF and Tree1m: there is a strong negative correlation (-0.626), suggesting that an increase in the proportion of trees leads to a reduction in sky visibility, which may affect people's perception of the environment and thermal comfort.
6. SVF and Grade: there is a significant negative correlation (-0.436), indicating that lower sky openness (i.e., more shading) might reduce perceived thermal comfort,

possibly because excessive shading reduces natural light, affecting thermal comfort perception.

7. Width and Grade: the correlation with most variables is low, suggesting that road width might not be a major factor influencing thermal comfort, or its impact is relatively smaller compared to other variables.

In summary, tree proportion, shadow coverage, green view index, and the sky view factor are key environmental factors affecting the thermal comfort of urban streets.

5. Discussion

5.1. The Importance of High-Precision Shadow Mapping for Assessing Thermal Comfort

When evaluating the thermal comfort of urban streets, precise shadow distribution is crucial. This study utilizes high-precision shadow mapping technology, offering a new perspective on urban microclimate effects. The accuracy of this method lies in its detailed depiction of shadow spatial distribution and its ability to capture dynamic changes over time. This spatiotemporal analysis capability is essential for accurately understanding thermal comfort at the street level.

Research by Huang and Wang has shown that high-resolution geospatial data significantly improve the accuracy of urban heat island effect assessments [36]. Similarly, this study emphasizes the importance of high-resolution imagery in capturing shadow changes in specific street areas. These changes, influenced by variations in the sun's altitude or the presence of buildings and vegetation, directly impact people's comfort. Buo et al. noted that shadows significantly reduce the heat load in urban environments [15], and high-precision mapping technology can detail how different buildings and natural features influence sunlight conditions. Furthermore, Park et al. demonstrated the powerful capabilities of shadow distribution visualization in modern urban planning [37]. By simulating and analyzing shadow distribution under different building and vegetation layouts, it is possible to predict the potential impact on thermal comfort during the early design stages. This predictive capability, often lacking in traditional methods, provides an effective tool for optimizing urban layouts to ensure maximum comfort in public spaces during hot seasons.

The application of this technology provides urban planners with concrete data to design more effective green spaces and building layouts for optimizing thermal comfort. By finely analyzing shadow distribution at different times of the day, planners can scientifically determine tree planting and building placements to maximize natural shading and reduce ground temperatures, thereby significantly enhancing the thermal comfort of urban spaces.

5.2. Comprehensive Analysis of Factors Affecting Urban Street Thermal Comfort

This study uses multiple linear regression analysis to reveal the main factors affecting the thermal comfort of urban streets, encompassing environmental, psychological, and functional dimensions.

Firstly, in the environmental dimension, the proportion of trees is an effective indicator related to the thermal environment. This study found that an increase in tree coverage significantly reduces street temperatures, consistent with findings by Han et al. [38], who noted that urban vegetation mitigates the urban heat island effect. Research by Sodoudi et al., Zölch et al., and Abdi et al. also supports that larger tree canopies have more significant cooling effects [39–41]. The proportion of buildings also positively impacts temperature by providing shade and regulating wind direction to improve thermal comfort, aligning with studies on urban morphology's influence on microclimate conditions [42,43].

Secondly, in the psychological dimension, GVI, SC, SVE, and Shade are important indicators. An increase in the GVI indicates more greenery, enriching the natural environment and positively affecting residents' psychological comfort. Shadow coverage and shading

status significantly lower air temperature, enhancing thermal comfort. Areas with higher SVF values offer a more open sky view, influencing residents' perception of thermal comfort. Both SVF and GVI, as key indicators of urban visual perception, play an important role in assessing thermal comfort [8]. High-precision shadow mapping technology, accurately capturing dynamic shadow changes, provides an essential perspective for understanding street sunlight conditions, crucial for evaluating urban street thermal comfort and offering new tools for urban planning.

Finally, in the functional dimension, the width of cycling and pedestrian paths significantly affects thermal comfort. Spacious paths not only improve traffic flow and convenience but also enhance the safety and comfort of users [44]. These wider paths can accommodate more shade and greenery, reducing the impact of direct sunlight and providing better thermal comfort.

5.3. Thermal Comfort Optimization Recommendations

In this study, we propose a comprehensive optimization plan for identified low-comfort areas to enhance the thermal comfort of urban streets and improve residents' quality of life. The plan is based on an in-depth environmental assessment and detailed surveys of community residents' needs, focusing on times of high pedestrian activity to ensure ample natural shade and a comfortable walking environment during these key periods.

Firstly, given this study's findings that tree canopy coverage within 10 m significantly reduces temperature, it is recommended to increase tree planting density in public spaces along streets [45]. In low-comfort areas, especially those with low shade coverage, high-shade tree species, should be planted. Wuhan is located in the northern subtropical monsoon humid climate zone. During the tree planting process, the summer and winter climate characteristics have been fully considered. The primary species that have been planted are deciduous broadleaf trees, with the main tree species being the French sycamore. For this climate type, particularly in areas with low temperatures in winter and high temperatures in summer, it is recommended to prioritize deciduous broadleaf forests. This approach not only enhances thermal comfort in the summer but also meets the need for sunlight in the winter. Other suitable deciduous broadleaf species for similar climate regions include ginkgo, maple, ash, and sycamore. These trees can provide ample shade and exhibit strong resistance to pollution and adaptability. These trees can provide sufficient shade during critical times, lower surface temperatures, and increase air humidity through transpiration. Additionally, creating green belts on both sides and in the center of streets by planting various plants, such as shrubs and flowers, can further enhance the GVI, improving the visual experience and psychological comfort of pedestrians.

Secondly, optimizing building layouts is an important regulatory measure. By adjusting the height and position of buildings, more shade can be provided during midday and afternoon, effectively reducing direct sunlight exposure. Transparent building designs with increased open spaces between structures can promote air circulation and reduce regional temperatures. Utilizing the shading effect of buildings can create cooler areas on streets, enhancing overall thermal comfort.

Increasing the GVI is another crucial approach to improving street comfort. Adding green belts and vertical greening, especially on building walls and roofs, can significantly enhance the GVI. Planting climbing plants and establishing rooftop gardens increases green landscapes, improving residents' visual comfort and psychological relaxation.

Reasonable use of the SVF is also key to optimizing street thermal comfort. By controlling the height and canopy width of trees to maintain adequate sky openness, streets can benefit from good natural light and air circulation while avoiding excessive obstruction

of the sky view. Adjusting tree planting density to maintain a proper SVF can help enhance overall environmental comfort.

Lastly, improving street infrastructure and amenities is a vital optimization measure. Installing shaded rest facilities such as benches and pavilions along streets provides resting spots for pedestrians. Optimizing the design of pedestrian and cycling paths by increasing their width ensures safety and comfort. Additionally, installing mist cooling systems on some streets can lower the surrounding temperature, enhancing pedestrian comfort.

Through these comprehensive measures, the thermal comfort of low-comfort street areas can be significantly improved, providing residents with a more livable environment. These strategies not only mitigate the urban heat island effect but also enhance the overall aesthetic and functionality of urban spaces.

5.4. Limitations of the Study

While this study provides in-depth insights into the relationship between urban street greening and residents' comfort, it also has limitations. Seasonal weather changes and leaf loss can cause variations in visible greenery levels at different locations. Additionally, the type of street trees, such as the height of the lowest branches and leaf density, may affect the relationship between GVI measured at human scale and satellite-based greening coverage. The method of collecting street view images also has limitations, as the perspective from a street view vehicle differs from a pedestrian's perspective and cannot access all areas, potentially leading to incomplete data and impacting the accuracy of the assessment.

Furthermore, pedestrian behavior patterns and differences in outdoor thermal comfort based on age or gender were not considered. Since people of different ages and genders have varying metabolic rates, residents may experience different levels of thermal comfort even when exposed to the same thermal environment.

6. Conclusions

This study comprehensively utilized the shadow and street view data of urban streets, combined with deep learning algorithms, integrating classic urban design elements with new urban data. It considered not only traditional physical and physiological factors but also incorporated analyses of social behavior characteristics and visual perceptions. This innovative, multi-dimensional, multi-scale, and multi-angle evaluation method provides a more comprehensive assessment of the thermal comfort of community streets in the summer.

By overcoming the limitations of traditional street view image analysis and emphasizing the combination of visual and practical aspects based on residents' daily lives, this approach offers robust scientific support for urban planning and policy-making. The results indicate that factors such as shade, SVF, and GVI significantly affect outdoor thermal comfort. Therefore, these factors should be thoroughly considered in policies and urban design to provide a more thermally comfortable environment. Additionally, during the renovation of existing streets, planting trees that provide shade and selecting appropriate leaf shapes are key to enhancing thermal comfort. This not only helps improve thermal comfort but also enhances the aesthetic and functional value of streets.

To further improve thermal comfort in summer urban areas, it is recommended that the government vigorously promote the development of horticulture and green buildings, encourage urban greening, and support the planning of greenways to ensure a comfortable thermal environment for pedestrians during the summer. Furthermore, strengthening the systematic planning of green spaces and streets, reducing the urban heat island effect, and enhancing residents' quality of life are core tasks for achieving sustainable urban development. Specifically, urban planners should prioritize the addition of trees and green belts in

streets and public spaces, especially in summer, to significantly reduce surface temperatures and improve thermal comfort by increasing tree canopy coverage and green space area. At the same time, policymakers should encourage the use of sustainable building materials, adjust building layouts, and design streets to ensure a reasonable distribution of shaded areas, thereby reducing the heat island effect. Moreover, the government should promote the development of green infrastructure, such as green roofs and permeable pavements, which will further optimize the urban environment. Through these comprehensive measures, not only can residents' thermal comfort needs in the summer be effectively met, but a solid foundation for sustainable urban development can also be established.

Author Contributions: Conceptualization, L.L.; methodology, L.L.; investigation, L.L.; data curation, X.W.; writing—original draft preparation, Y.N.; writing—review and editing, L.L.; visualization, Y.N.; supervision, H.X.; funding acquisition, L.L.; validation, X.W. All authors have read and agreed to the published version of the manuscript.

Funding: This research was supported by the National Natural Science Foundation of China (Grant No. 32001368).

Institutional Review Board Statement: Not applicable.

Informed Consent Statement: Not applicable.

Data Availability Statement: The data presented in this study are available upon reasonable request to the corresponding author.

Acknowledgments: The authors would like to thank the editors and reviewers for providing their valuable comments and suggestions.

Conflicts of Interest: The authors declare no conflicts of interest.

References

1. Larrañaga, A.M.; Rizzi, L.I.; Arellana, J.; Strambi, O.; Cybis, H.B.B. The Influence of Built Environment and Travel Attitudes on Walking: A Case Study of Porto Alegre, Brazil. *Int. J. Sustain. Transp.* **2016**, *10*, 332–342. [[CrossRef](#)]
2. Guzman, L.A.; Arellana, J.; Castro, W.F. Desirable Streets for Pedestrians: Using a Street-Level Index to Assess Walkability. *Transp. Res. Part D Transp. Environ.* **2022**, *111*, 103462. [[CrossRef](#)]
3. Zhao, H.; Zhao, L.; Zhai, Y.; Jin, L.; Meng, Q.; Yan, J.; Wu, R.; Brown, R.D. The Impact of Dynamic Thermal Experiences on Pedestrian Thermal Comfort: A Whole-Trip Perspective from Laboratory Studies. *Build. Environ.* **2024**, *258*, 111599. [[CrossRef](#)]
4. Heaviside, C.; Vardoulakis, S.; Cai, X.-M. Attribution of Mortality to the Urban Heat Island during Heatwaves in the West Midlands, UK. *Environ. Health* **2016**, *15*, S27. [[CrossRef](#)]
5. Ashrae, A. *Standard 55-2020: Thermal Environmental Conditions for Human Occupancy*; American Society of Heating, Refrigerating, and Air-Conditioning Engineers, Inc.: Atlanta, GA, USA, 2020.
6. Gong, F.-Y.; Zeng, Z.-C.; Zhang, F.; Li, X.; Ng, E.; Norford, L.K. Mapping Sky, Tree, and Building View Factors of Street Canyons in a High-Density Urban Environment. *Build. Environ.* **2018**, *134*, 155–167. [[CrossRef](#)]
7. Zhang, J.; Guo, W.; Cheng, B.; Jiang, L.; Xu, S. A Review of the Impacts of Climate Factors on Humans' Outdoor Thermal Perceptions. *J. Therm. Biol.* **2022**, *107*, 103272. [[CrossRef](#)] [[PubMed](#)]
8. Zhou, H.; Tao, G.; Nie, Y.; Yan, X.; Sun, J. Outdoor Thermal Environment on Road and Its Influencing Factors in Hot, Humid Weather: A Case Study in Xuzhou City, China. *Build. Environ.* **2022**, *207*, 108460. [[CrossRef](#)]
9. Chun, B.; Guldmann, J.-M. Impact of Greening on the Urban Heat Island: Seasonal Variations and Mitigation Strategies. *Comput. Environ. Urban Syst.* **2018**, *71*, 165–176. [[CrossRef](#)]
10. Li, T.; Zheng, X.; Wu, J.; Zhang, Y.; Fu, X.; Deng, H. Spatial Relationship between Green View Index and Normalized Differential Vegetation Index within the Sixth Ring Road of Beijing. *Urban For. Urban Green.* **2021**, *62*, 127153. [[CrossRef](#)]
11. Xia, Y.; Yabuki, N.; Fukuda, T. Development of a System for Assessing the Quality of Urban Street-Level Greenery Using Street View Images and Deep Learning. *Urban For. Urban Green.* **2021**, *59*, 126995. [[CrossRef](#)]
12. Yang, Y.; Zhou, D.; Gao, W.; Zhang, Z.; Chen, W.; Peng, W. Simulation on the Impacts of the Street Tree Pattern on Built Summer Thermal Comfort in Cold Region of China. *Sustain. Cities Soc.* **2018**, *37*, 563–580. [[CrossRef](#)]
13. Gehl, J. *Life Between Buildings: Using Public Space*; Van Nostrand Reinhold: New York, NY, USA, 1987; pp. 54–55.

14. Gupta, K.; Kumar, P.; Pathan, S.K.; Sharma, K.P. Urban Neighborhood Green Index—A Measure of Green Spaces in Urban Areas. *Landsc. Urban Plan.* **2012**, *105*, 325–335. [[CrossRef](#)]
15. Buo, I.; Sagris, V.; Jaagus, J.; Middel, A. High-Resolution Thermal Exposure and Shade Maps for Cool Corridor Planning. *Sustain. Cities Soc.* **2023**, *93*, 104499. [[CrossRef](#)]
16. Aminipouri, M.; Rayner, D.; Lindberg, F.; Thorsson, S.; Knudby, A.J.; Zickfeld, K.; Middel, A.; Krayenhoff, E.S. Urban Tree Planting to Maintain Outdoor Thermal Comfort under Climate Change: The Case of Vancouver’s Local Climate Zones. *Build. Environ.* **2019**, *158*, 226–236. [[CrossRef](#)]
17. Wu, S.; Yu, W.; Chen, B. Observed Inequality in Thermal Comfort Exposure and Its Multifaceted Associations with Greenspace in United States Cities. *Landsc. Urban Plan.* **2023**, *233*, 104701. [[CrossRef](#)]
18. Balslev, Y.J.; Potchter, O.; Matzarakis, A. Climatic and Thermal Comfort Analysis of the Tel-Aviv Geddes Plan: A Historical Perspective. *Build. Environ.* **2015**, *93*, 302–318. [[CrossRef](#)]
19. Hiemstra, J.A.; Saaroni, H.; Amorim, J.H. The Urban Heat Island: Thermal Comfort and the Role of Urban Greening. In *The Urban Forest: Cultivating Green Infrastructure for People and the Environment*; Pearlmutter, D., Calfapietra, C., Samson, R., O’Brien, L., Krajter Ostoić, S., Sanesi, G., Alonso del Amo, R., Eds.; Springer International Publishing: Cham, Switzerland, 2017; pp. 7–19.
20. Middel, A.; Selover, N.; Hagen, B.; Chhetri, N. Impact of Shade on Outdoor Thermal Comfort—A Seasonal Field Study in Tempe, Arizona. *Int. J. Biometeorol.* **2016**, *60*, 1849–1861. [[CrossRef](#)] [[PubMed](#)]
21. Handy, S.L.; Boarnet, M.G.; Ewing, R.; Killingsworth, R.E. How the Built Environment Affects Physical Activity: Views from Urban Planning. *Am. J. Prev. Med.* **2002**, *23*, 64–73. [[CrossRef](#)]
22. Jamei, E.; Rajagopalan, P. Urban Development and Pedestrian Thermal Comfort in Melbourne. *Sol. Energy* **2017**, *144*, 681–698. [[CrossRef](#)]
23. Speak, A.; Montagnani, L.; Wellstein, C.; Zerbe, S. Forehead Temperatures as an Indicator of Outdoor Thermal Comfort and the Influence of Tree Shade. *Urban Clim.* **2021**, *39*, 100965. [[CrossRef](#)]
24. Wallenberg, N.; Lindberg, F.; Rayner, D. Locating Trees to Mitigate Outdoor Radiant Load of Humans in Urban Areas Using a Metaheuristic Hill-Climbing Algorithm—Introducing TreePlanter v1.0. *Geosci. Model Dev.* **2022**, *15*, 1107–1128. [[CrossRef](#)]
25. Armson, D.; Stringer, P.; Ennos, A.R. The Effect of Tree Shade and Grass on Surface and Globe Temperatures in an Urban Area. *Urban For. Urban Green.* **2012**, *11*, 245–255. [[CrossRef](#)]
26. Rahman, M.A.; Moser, A.; Gold, A.; Rötzer, T.; Pauleit, S. Vertical Air Temperature Gradients under the Shade of Two Contrasting Urban Tree Species during Different Types of Summer Days. *Sci. Total Environ.* **2018**, *633*, 100–111. [[CrossRef](#)]
27. Chinchilla, J.; Carbonnel, A.; Galleguillos, M. Effect of Urban Tree Diversity and Condition on Surface Temperature at the City Block Scale. *Urban For. Urban Green.* **2021**, *60*, 127069. [[CrossRef](#)]
28. Viana-Fons, J.D.; González-Maciá, J.; Payá, J. Development and Validation in a 2D-GIS Environment of a 3D Shadow Cast Vector-Based Model on Arbitrarily Orientated and Tilted Surfaces. *Energy Build.* **2020**, *224*, 110258. [[CrossRef](#)]
29. Lin, L.; Deng, Y.; Peng, M.; Zhen, L.; Qin, S. Multi-Scale Influence Analysis of Urban Shadow and Spatial Form Features on Urban Thermal Environment. *Remote Sens.* **2023**, *15*, 4902. [[CrossRef](#)]
30. Lindberg, F.; Grimmond, C.S.B.; Gabey, A.; Huang, B.; Kent, C.W.; Sun, T.; Theeuwes, N.E.; Jarvi, L.; Ward, H.C.; Capel-Timms, I.; et al. Urban Multi-Scale Environmental Predictor (UMEP): An Integrated Tool for City-Based Climate Services. *Environ. Model. Softw.* **2018**, *99*, 70–87. [[CrossRef](#)]
31. Lan, Y.; Zhan, Q. How Do Urban Buildings Impact Summer Air Temperature? The Effects of Building Configurations in Space and Time. *Build. Environ.* **2017**, *125*, 88–98. [[CrossRef](#)]
32. Yu, H.; Yang, Z.; Tan, L.; Wang, Y.; Sun, W.; Sun, M.; Tang, Y. Methods and Datasets on Semantic Segmentation: A Review. *Neurocomputing* **2018**, *304*, 82–103. [[CrossRef](#)]
33. Li, X.; Zhang, C.; Li, W.; Ricard, R.; Meng, Q.; Zhang, W. Assessing Street-Level Urban Greenery Using Google Street View and a Modified Green View Index. *Urban For. Urban Green.* **2015**, *14*, 675–685. [[CrossRef](#)]
34. Orihara, N. Study on the evaluation of green landscapes: Consideration of green evaluation methods for good landscape formation. *Build. Environ. Energy Conserv. Inf.* **2006**, *27*, 32–35.
35. Jenks, G. The Data Model Concept in Statistical Mapping. *Int. Yearb. Cartogr.* **1967**, *7*, 186–190.
36. Huang, X.; Wang, Y. Investigating the Effects of 3D Urban Morphology on the Surface Urban Heat Island Effect in Urban Functional Zones by Using High-Resolution Remote Sensing Data: A Case Study of Wuhan, Central China. *ISPRS J. Photogramm. Remote Sens.* **2019**, *152*, 119–131. [[CrossRef](#)]
37. Park, Y.; Zhao, Q.; Guldmann, J.-M.; Wentz, E.A. Quantifying the Cumulative Cooling Effects of 3D Building and Tree Shade with High Resolution Thermal Imagery in a Hot Arid Urban Climate. *Landsc. Urban Plan.* **2023**, *240*, 104874. [[CrossRef](#)]
38. Han, L.; Zhang, R.; Wang, J.; Cao, S.-J. Spatial Synergistic Effect of Urban Green Space Ecosystem on Air Pollution and Heat Island Effect. *Urban Clim.* **2024**, *55*, 101940. [[CrossRef](#)]
39. Sodoudi, S.; Zhang, H.; Chi, X.; Müller, F.; Li, H. The Influence of Spatial Configuration of Green Areas on Microclimate and Thermal Comfort. *Urban For. Urban Green.* **2018**, *34*, 85–96. [[CrossRef](#)]

40. Zölch, T.; Rahman, M.A.; Pfliederer, E.; Wagner, G.; Pauleit, S. Designing Public Squares with Green Infrastructure to Optimize Human Thermal Comfort. *Build. Environ.* **2019**, *149*, 640–654. [[CrossRef](#)]
41. Abdi, B.; Hami, A.; Zarehaghi, D. Impact of Small-Scale Tree Planting Patterns on Outdoor Cooling and Thermal Comfort. *Sustain. Cities Soc.* **2020**, *56*, 102085. [[CrossRef](#)]
42. Oke, T.R. The Energetic Basis of the Urban Heat Island. *Q. J. R. Meteorol. Soc.* **1982**, *108*, 1–24. [[CrossRef](#)]
43. Kim, Y.-H.; Baik, J.-J. Spatial and Temporal Structure of the Urban Heat Island in Seoul. *J. Appl. Meteorol. Climatol.* **2005**, *44*, 591–605. [[CrossRef](#)]
44. Rodríguez, D.A.; Brisson, E.M.; Estupiñán, N. The Relationship between Segment-Level Built Environment Attributes and Pedestrian Activity around Bogota's BRT Stations. *Transp. Res. Part D Transp. Environ.* **2009**, *14*, 470–478. [[CrossRef](#)]
45. Azcarate, I.; Acero, J.Á.; Garmendia, L.; Rojí, E. Tree Layout Methodology for Shading Pedestrian Zones: Thermal Comfort Study in Bilbao (Northern Iberian Peninsula). *Sustain. Cities Soc.* **2021**, *72*, 102996. [[CrossRef](#)]

Disclaimer/Publisher's Note: The statements, opinions and data contained in all publications are solely those of the individual author(s) and contributor(s) and not of MDPI and/or the editor(s). MDPI and/or the editor(s) disclaim responsibility for any injury to people or property resulting from any ideas, methods, instructions or products referred to in the content.